nature communications

Article

https://doi.org/10.1038/s41467-025-67771-9

Informationally complete distributed metrology without a shared reference frame

Received: 7 May 2025

Accepted: 8 December 2025

Published online: 24 December 2025

Check for updates

Hua-Qing Xu[1,2,3,4,5], Gong-Chu Li[1,2,3,4,5], Xu-Song Hong[1,2,3], Lei Chen[1,2,3], Si-Qi Zhang[1,2,3], Yuancheng Liu[1,2], Geng Chen[1,2,3,4] ✉, Chuan-Feng Li[1,2,3,4] & Guang-Can Guo[1,2,3,4]

In quantum information processing, implementing arbitrary preparations and measurements on qubits necessitates precise information to identify a specific reference frame (RF). In space quantum communication and sensing, where a shared RF is absent, the interplay between locality and symmetry imposes fundamental restrictions on physical systems. A restriction on realizable unitary operations results in a no-go theorem prohibiting the extraction of locally encoded information in RF-independent distributed metrology. Here, we propose a reversed-encoding method applied to two copies of local-unitary-invariant network states. This approach circumvents the no-go theorem while simultaneously mitigating decoherence-like noise caused by RF misalignment, thereby enabling the complete recovery of the quantum Fisher information (QFI). Furthermore, we confirm local Bell-state measurements as an optimal strategy to saturate the QFI. Our findings pave the way for the field application of distributed quantum sensing, which is inherently subject to unknown RF misalignment and was previously precluded by the no-go theorem.

In classical information theory, Shannon's coding theorems are indifferent to means of encoding, rendering the value of the classical bit fungible, which suffices for various information processing tasks, such as data compression, key distribution, or integer factoring[1]. The quantum analogs of these tasks might appear to require only the fungible information of qubits. However, this is not the case in quantum information processing, as accessing fungible information demands the selection of specific degrees of freedom for implementing arbitrary preparations and measurements. In other words, the identification of the reference frame (RF) serves as the infungible information. For simplicity, most quantum information protocols assume that the involved parties share a common RF. Nevertheless, this assumption often fails in distributed quantum tasks, ranging from space interferometry—where a network of sensors measures a single global parameter from a distant source[2,3], to creating a 'world clock' by synchronizing sensors that each measure an independent local parameter[4]. In such scenarios, distributed quantum networks promise precision scaling with the number of sites (N), as $1/N$ (the Heisenberg limit, HL), surpassing the $1/\sqrt{N}$ standard quantum limit (SQL) of independent sensors[5–11]. The absence of a shared RF, however, is a primary obstacle to achieve this quantum-enhanced precision.

The role of RF in quantum information processing is closely tied to two essential properties of the physical world: locality and symmetry. Their interplay imposes fundamental restrictions on physical systems. A fundamental restriction revealed by Iman Marvian is that[12]: generic symmetric unitaries cannot be implemented, even approximately, using local symmetric unitaries. For RF-independent metrology, this restriction manifests as a no-go theorem: if a parameter-encoding process is locally constructible (i.e., realizable by a sequence of local symmetric operations), the encoded information will be completely erased by RF misalignment. This no-go theorem renders the field application of distributed metrology protocols an intractable task, such as satellite-based network sensing.

[1]Laboratory of Quantum Information, University of Science and Technology of China, Hefei, China. [2]Anhui Province Key Laboratory of Quantum Network, Hefei, Anhui, China. [3]CAS Center For Excellence in Quantum Information and Quantum Physics, University of Science and Technology of China, Hefei, Anhui, China. [4]Hefei National Laboratory, Hefei, China. [5]These authors contributed equally: Hua-Qing Xu, Gong-Chu Li. ✉e-mail: chengeng@ustc.edu.cn

Another challenge for RF-independent metrology is that the RF misalignment can be modeled as a *superselection rule* or an effective *decoherence* noise[1], which is particularly detrimental to quantum sensing[13–21] and devastate the quantum advantages[22–24]. In principle, aligning the RFs could obviate this noise; however, this may not be feasible for time-sensitive quantum tasks and often requires additional resources and communication overhead[1]. Quantum error correction code[25–28] or decoherence-free subspaces can also mitigate this decoherence noise[1], but the experimental complexity impedes the flexibility and universality of these protocols.

A recent study proposed that utilizing multiple copies of a quantum state can effectively mitigate the decoherence-like effect arising from RF misalignment[29], thereby enabling the estimation of a global parameter in an RF-independent configuration when it is linked to the properties of entangled states. However, this approach remains fundamentally constrained by the limitations of the no-go theorem. Simply protecting the state is not enough; one must still be able to encode a parameter onto it. This leaves a critical gap: a method is needed that not only protects the state from RF-induced noise but also provides a valid mechanism for local information encoding that circumvents the no-go theorem.

In this work, we develop a framework to address the crucial challenges for distributed metrology when lacking a shared RF, thereby the no-go theorem can be effectively circumvented and the encoded parameters can be accessed with local operations. Specifically, we introduce a protocol termed 2-LUI-RE, which employs reversed encoding on two copies of a local unitary invariant (LUI) network state. Fisher information analysis reveals that 2-LUI-RE could fully recover the quantum Fisher information (QFI) and preserve Heisenberg-limited scaling, provided the sites share a Greenberger-Horne-Zeilinger (GHZ) state. Furthermore, we show that local Bell-state measurements (LBM) constitute the optimal measurement strategy for saturating the QFI, whereas standard randomized measurements suffer an exponential loss of information.

Results

The role of RF in distributed quantum network

The orientation of any classical object is defined relative to a local RF. When viewed from a different, global RF, this local frame appears to be rotated. Any such misalignment between a local and a global frame can be described by an element of the rotation group, SO(3), representing a physical rotation in three-dimensional space (Fig. 1a). Similarly, in distributed systems, the mismatch between the local RF at the i-th site and a chosen global RF is described by a rotation $g_i \in \mathrm{SO}(3)$.

Accurate knowledge of the RF alignment is also a prerequisite for quantum information processing tasks. Quantum states are invariably defined with respect to the same local RF as the classical apparatus used to prepare and measure them. For instance, in photonic systems, the RF is typically defined relative to the optical table: horizontal polarization ($|H\rangle$) refers to polarization parallel to the table surface, and vertical polarization ($|V\rangle$) refers to polarization perpendicular to it, assuming the propagation direction lies along the plane of the table[30]. A qubit state defined by polarizations at the i-th site viewed by itself can be written as $|\psi\rangle = \alpha_i|H_i\rangle + \beta_i|V_i\rangle$, where $|H_i\rangle$ and $|V_i\rangle$ denote the local horizontal and vertical polarizations. From a global reference point, this state appears as a different state which has been rotated via a unitary transformation $\widehat{V}_i(g_i) \in SU(2)$, such that $|H\rangle = \widehat{V}_i(g_i)|H_i\rangle$ and $|V\rangle = \widehat{V}_i(g_i)|V_i\rangle$[1]. This mapping, $\widehat{V}_i : SO(3) \to SU(d)$ is related to the specific experimental arrangement and provides the intrinsic connection between a physical rotation of the classical apparatus and the

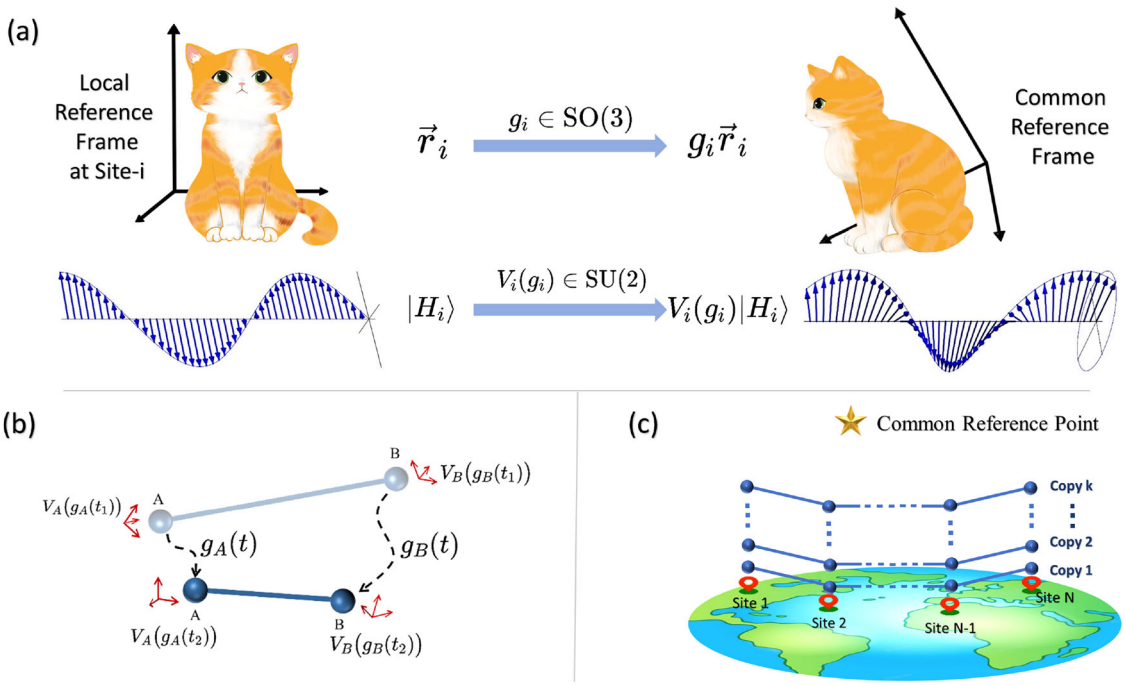

Fig. 1 | The Role of RFs and the Impact of Their Misalignment in Quantum Information Processing. a Demonstration of RF Misalignment for Classical and Quantum Objects. The left side shows objects defined in a local RF at Site-i, while the right side shows the same objects as viewed from a common RF. For a classical object (upper), e.g., a cat, a misalignment between frames is described by a 3D rotation $g_i \in \mathrm{SO}(3)$. An orientation vector $\vec{\mathbf{r}}_i$ in the local frame is perceived as $g_i\vec{\mathbf{r}}_i$ in the common frame. For a quantum object (down), such as a photon in a horizontally-polarized state $|H_i\rangle$, the same physical rotation corresponds to a transformation $\widehat{V}_i(g_i) \in SU(2)$ on its quantum state. This results in a different state, such as an elliptical polarization, in the common frame. **b** Demonstration of the Effects of Drifting RFs on the State Shared in Two Sites. From the view of the common reference point, the coordination of site A and B is changing with $g_A(t), g_B(t) \in \mathrm{SO}(3)$. The corresponding shared state ρ_{AB} is experiencing the unitary rotation given $\widehat{V}_A(g_A) \otimes \widehat{V}_B(g_B)$. The average effect over the measuring time is the G-twirling. **c** Demonstration of k-copy Quantum States Shared in N sites. The connected dots represent an N-qudit state shared in N sites. And the shared k copies mean that kN-qudit states are included. At each site, there are k qudits (k balls), one for each copy.

corresponding unitary transformation on the quantum state's Hilbert space[1].

Decoherence-like Noise by RF misalignment

In dynamic scenarios—e.g., satellite-based quantum networks—RFs may fluctuate with time, modeled as $g_i(t)$ (shown in Fig. 1b). For a system consist of two sites − A and B, from a fixed reference point, the effective state over a time interval is given by the averaged state $\rho_{AB,g} = \int dg_A dg_B \hat{V}_A(g_A) \otimes \hat{V}_B(g_B) \rho_{AB} \hat{V}_A(g_A)^\dagger \otimes \hat{V}_B(g_B)^\dagger = \mathcal{G}(\rho_{AB})$. The averaging process, denoted $\mathcal{G}$, is known as a G-twirling channel[1]. For a general N-site state ρ, the misalignment is described by a vector of rotations $\vec{\mathbf{g}} = (g_1, g_2, ..., g_N)$, and the twirled state is $\mathcal{G}(\rho) = \int d\vec{\mathbf{g}} \hat{V}(\vec{\mathbf{g}}) \rho \hat{V}(\vec{\mathbf{g}})^\dagger$, where $\hat{V}(\vec{\mathbf{g}}) = \hat{V}_1(g_1) \otimes \cdots \otimes \hat{V}_N(g_N)$. In the extreme case where the local rotations are uniformly distributed over the Haar measure, this G-twirling operation becomes a full depolarization channel, mapping any input state to the maximally mixed state, $\mathcal{G}(\rho) = \hat{I}/d^N$, and thereby erasing all initial information.

Fortunately, the effect of RF misalignment can be transformed by sharing multiple copies of a state across sites. When k copies of the state are distributed across N sites, the whole k-copy state can be expressed as $\rho^{\otimes k}$ with each ρ an N-qudit state (shown in Fig. 1c). When k copies are shared, we assume that all k qudits at a given site share a common local RF. Consequently, an RF misalignment at site i subjects all k copies to an identical, collective unitary rotation, $\hat{V}_i(g_i)^{\otimes k}$. The total effective state, averaged over all misalignments, is given by the k-copy G-twirling channel, $\mathcal{G}^{(k)}(\rho^{\otimes k}) = \int d\vec{\mathbf{g}} \hat{V}(\vec{\mathbf{g}})^{\otimes k} \rho^{\otimes k} \hat{V}(\vec{\mathbf{g}})^{\dagger \otimes k}$. Crucially, for $k \geq 2$, this channel is no longer a simple depolarization. Instead, $\mathcal{G}^{(k)}$ acts as a projection onto the subspace of operators invariant under collective local rotations.

No-go theorem on distributed quantum sensing

Distributed quantum sensing is inherently associated with two essential properties of the physical world: locality and symmetry, and is therefore subject to the fundamental limitation proposed in ref. 12. Such a limitation defines the implementability of generic symmetric untiaries, stating as: in the continuous system like SU(2), if a unitary $\hat{U} \notin \mathcal{U}_l^G$, then it cannot be implemented using l-local symmetric unitaries; on the other hand, if $\hat{U} \in \mathcal{U}_l^G$, then it can be implemented with a uniformly finite number of such unitaries[12,31]. Here, $\mathcal{U}_l^G$ represents the set of all unitary operations obeying a global symmetry that can be generated using interactions acting on at most l sites, which can be expressed as $\mathcal{U}_l^G = \{\hat{U} \in l\text{-local unitary} | [\hat{U}, \hat{V}(\vec{\mathbf{g}})] = 0, \forall \vec{\mathbf{g}} \in G\}$, forming a connected and compact Lie group and a closed manifold. Marvian also states that the "reach" of these operations, measured by the dimension of their manifold (as 'dim' below), strictly increases with the l-locality, $\dim(\mathcal{U}_l^G) > \dim(\mathcal{U}_{l'}^G)$ if $l > l'$.

The absence of a shared RF imposes such a symmetry: a physically non-trivial implementable encoding should respect unknown 3D space rotations described by SO(3). Applying Marvian's restriction to RF-independent scenarios results in a no-go theorem, which states that any information encoded through a 1-local process is completely erased under RF-averaging. Consequently, the accessible information has to be encoded in the set of operations that can only be implemented via non-local approaches, which features $l \geq 2$.

This stringent constraint applies directly when operations are identical across multiple copies, as the overall process remains symmetric. However, the multi-copy framework itself introduces a new physical resource: the ability to apply distinct or correlated operations to each copy. This breaks the SWAP symmetry in copy space, providing a potential pathway to encode information using only local site operations ($l = 1$) while circumventing the no-go theorem's core symmetry assumption. More discussions are provided in Supplementary Note I.

Mitigating RF decoherence with multi-copy twirling

Based on the above discussion, we conclude that all effects of RFs are generated by local SU(d) unitaries. And the effect of RF-misalignment acts as a decoherence-like noise described by G-twirling. Thus, for a state to be invariant in the RF-independent case, it must be LUI. The group of transformations corresponding to RF misalignment for k-copies shared among N sites is therefore $\mathcal{V}_k = \{\hat{V}^{\otimes k} | \hat{V} \in SU(d)^{\otimes N}\}$[1,29]. A state $\tilde{\rho}$ is a k-copy LUI state if it is a fixed point of this group of operations: $\hat{V}_k \tilde{\rho} \hat{V}_k^\dagger = \tilde{\rho}$ for all $\hat{V}_k \in \mathcal{V}_k$.

A general method to construct an LUI state from an arbitrary initial state is to average it over all possible local orientations. This process, known as k-twirling for k copies, projects the state into the RF-invariant subspace, rendering the averaged state immune to subsequent RF noise. Specifically, the local k-twirling channel at site-i is defined as: $\Phi_i^{(k)}(\cdot) = \int_{Haar} d\hat{U}_i \hat{U}_i^{\otimes k} (\cdot) \hat{U}_i^{\dagger \otimes k}$, where the integral is over the Haar measure of SU(d)[32,33].

By applying this channel to each site, $\Phi_{local}^{(k)} = \bigotimes_{i=1}^N \Phi_i^{(k)}$, we project the initial k-copy state into the LUI subspace, $\tilde{\rho} = \Phi_{local}^{(k)}(\rho^{\otimes k})$. By construction, the resulting mixed state is invariant under decoherence-noise by any RF misalignment, i.e., G-twirling,

$$\tilde{\rho} = \mathcal{G}^{(k)}(\tilde{\rho}), \forall \mathcal{G}^{(k)}. \tag{1}$$

For the single-copy case ($k = 1$), this projection is trivial, yielding the maximally mixed state $\tilde{\rho} = \hat{I}/d^N$. However, for $k \geq 2$, the LUI subspace is non-trivial and can support quantum information.

For quantum metrology, we consider the LUI states are constructed from independent encoded states $\rho_{j,\theta}$ where $j = 1, \cdots, k$ indexes the copy. With the encoding process for each copy as $\rho_{j,\theta} = \Theta_{j,\theta} \rho_0 \Theta_{j,\theta}^\dagger$, the encoded LUI states are

$$\tilde{\rho}_\theta = \Phi_{local}^{(k)}(\rho_{1,\theta} \otimes \cdots \otimes \rho_{k,\theta}). \tag{2}$$

The explicit form of the k-twirling channel can be derived using Schur-Weyl duality, which decomposes the k-fold Hilbert space $\mathcal{H}^{\otimes k}$ into invariant subspaces under the joint action of the unitary and symmetric groups[34]. For general $O \in \mathbb{C}^{d^k \times d^k}$, the twirling map takes the form $\Phi^{(k)}(O) = \sum_{\sigma,\pi \in S_k} c_{\sigma,\pi} Tr(O W_\sigma) W_\pi$, where S_k is the permutation group, W_σ and W_π denote the permutation operators corresponding to σ and π respectively, and $c_{\sigma,\pi}$ are Weingarten coefficients[32,33].

The two-copy case ($k = 2$) is the minimal non-trivial paradigm to preserve the Fisher information in the absence of a shared RF. For $k = 2$, the resulting state lies in the symmetric and antisymmetric subspaces spanned by the identity and SWAP operators. The SWAP operator $\hat{S}$ acts as $\hat{S}|\psi_1\rangle|\psi_2\rangle = |\psi_2\rangle|\psi_1\rangle$. To be specific, arbitrary matrix O with $Tr(O) = 1$ after the 2-twirling channel satisfies:

$$\Phi^{(2)}(O) = \frac{1}{d^2 - 1}(\hat{S} + Tr(\hat{S}O))(\hat{S} - \hat{I}/d). \tag{3}$$

Let the 2-copy initial encoded state be $\rho_{1,\theta}$ and $\rho_{2,\theta}$, denoting two identical N-particle states parameterized by θ, each defined on a d-dimensional local Hilbert space. Define $P_\theta := \rho_{1,\theta} \otimes \rho_{2,\theta}$. The corresponding LUI state is obtained by applying a local 2-twirling channel, which can be implemented locally. The channel factorizes as $\Phi_{local}^{(2)} = \bigotimes_{i=1}^N \Phi_i^{(2)}$, where each $\Phi_i^{(2)}$ acts locally on the i-th site. The resulting LUI state becomes

$$\tilde{\rho}_\theta = \left(\frac{1}{d^2 - 1}\right)^N \sum_{\vec{\mathbf{a}}} Tr(\hat{S}_{\vec{\mathbf{a}}} P_\theta) \bigotimes_{i:a_i=0} \hat{A}_i \bigotimes_{j:a_j=1} \hat{B}_j, \tag{4}$$

where $\vec{\mathbf{a}}$ is an N-bit binary string, and $\hat{S}_{\vec{\mathbf{a}}} := \bigotimes_{i:a_i=1} \hat{S}_i$ with $\hat{S}_i$ the local SWAP acting on the i-th site. The operators $\hat{A}_i := \hat{I}_i - \hat{S}_i/d$ and $\hat{B}_i := \hat{S}_i - \hat{I}_i/d$ define two local subspaces. Further details are provided in Supplementary Note II.

Eq. (4) shows that the LUI state retains nontrivial dependence on θ via $Tr(\hat{S}_{\vec{\mathbf{a}}} P_\theta)$, in contrast to the trivial case of a single-copy state. Moreover, the structure of the retained information depends on the encoding strategy.

Circumventing the No-go theorem with 2-LUI-RE protocol

In this subsection, we propose a strategy to circumvent the no-go theorem in RF-independent distributed quantum sensing by breaking the SWAP symmetry between the two copies.

For a two-copy LUI state, there are two instinct encoding strategies: (1) Identical Encoding (IE): Following ref. 29, both copies are prepared identically: $P_\theta = \rho_\theta \otimes \rho_\theta$. This construction is manifestly SWAP-symmetric in copy space, i.e. $Tr(\hat{S}P_\theta) = 1$. (2) Reversed Encoding (RE): Our proposed strategy prepares the copies with opposite encodings: $P_\theta = \rho_\theta \otimes \rho_{-\theta}$. This process explicitly breaks the SWAP symmetry in copy space, i.e., $Tr(\hat{S}P_\theta)$ is related to θ, which, as we will show, is the key to its enhanced metrological power.

To study the metrological advantages of the two strategies, we take rigorous Fisher information analysis. Before proceeding, we briefly review quantum metrology[15]. In quantum parameter estimation, where θ is encoded in the state $\tilde{\rho}_\theta$, the quantum Cramér-Rao bound (QCRB) sets a lower bound on the estimation uncertainty[35]:

$$\Delta\theta \geq \frac{1}{\sqrt{\nu F}} \geq \frac{1}{\sqrt{\nu \mathcal{F}}} \geq \frac{1}{\sqrt{\nu \mathcal{F}_{\max}}}. \tag{5}$$

Here, F is the classical Fisher information (CFI), dependent on the measurement M, encoding Hamiltonian $\hat{H}$, and input state ρ_0. The QFI, $\mathcal{F}$, is the CFI optimized over all measurements, while $\mathcal{F}_{\max} = \max_{\rho_0} \mathcal{F}$ is optimized over probe states and depends solely on the encoding.

The QFI can be computed from the encoded state ρ_θ via the symmetric logarithmic derivative (SLD) $\hat{L}_\theta$ satisfying $\partial_\theta \rho_\theta = \frac{1}{2}(\rho_\theta \hat{L}_\theta + \hat{L}_\theta \rho_\theta)$, yielding $\mathcal{F} = Tr(\rho_\theta \hat{L}_\theta^2)$[36]. For general mixed states $\tilde{\rho}_\theta = \sum_m \lambda_m |\psi_m\rangle\langle\psi_m|$, the QFI is given by

$$\mathcal{F} = \sum_m \frac{(\partial_\theta \lambda_m)^2}{\lambda_m} + 2\sum_{m,n} \frac{(\lambda_m - \lambda_n)^2}{\lambda_m + \lambda_n} |\langle \partial_\theta \psi_m | \psi_n \rangle|^2, \tag{6}$$

where the summations exclude terms with $\lambda_m = 0$ or $\lambda_m + \lambda_n = 0$. Since all LUI states are linear combinations of permutation operators (per Eq. (4)), their eigenstates are θ-independent, and only the first term contributes in Eq. (6).

In the identical encoding strategy, called 2-LUI-IE protocol, as shown in Fig. 2a, the QFI is determined by the eigenvalues of $\tilde{\rho}_\theta$. We denote symmetric or antisymmetric subspaces by a binary vector $\vec{\mathbf{b}}$, and define $\rho_{\theta,\vec{\mathbf{a}}} := Tr_{i:a_i=0}(\rho_\theta)$. The QFI reads

$$\mathcal{F}_{2-\mathrm{LUI-IE}} = \frac{1}{2^N} \sum_{\vec{\mathbf{b}}} \frac{\left[\sum_{\vec{\mathbf{a}}} (-1)^{\vec{\mathbf{a}}\cdot\vec{\mathbf{b}}} \partial_\theta Tr(\rho^2_{\theta,\vec{\mathbf{a}}})\right]^2}{\sum_{\vec{\mathbf{a}}} (-1)^{\vec{\mathbf{a}}\cdot\vec{\mathbf{b}}} Tr(\rho^2_{\theta,\vec{\mathbf{a}}})}. \tag{7}$$

is related to the 2-Renyi entropy of the subsystem $\hat{B}$ (sites with $a_i = 1$). Thus, as derived in Supplementary Note III, this QFI is sensitive to the entanglement properties of ρ_θ. Notably, for $\rho_\theta = \Theta_\theta \rho_0 \Theta_\theta^\dagger$, when the encoding operation involves only local interactions - expressed as

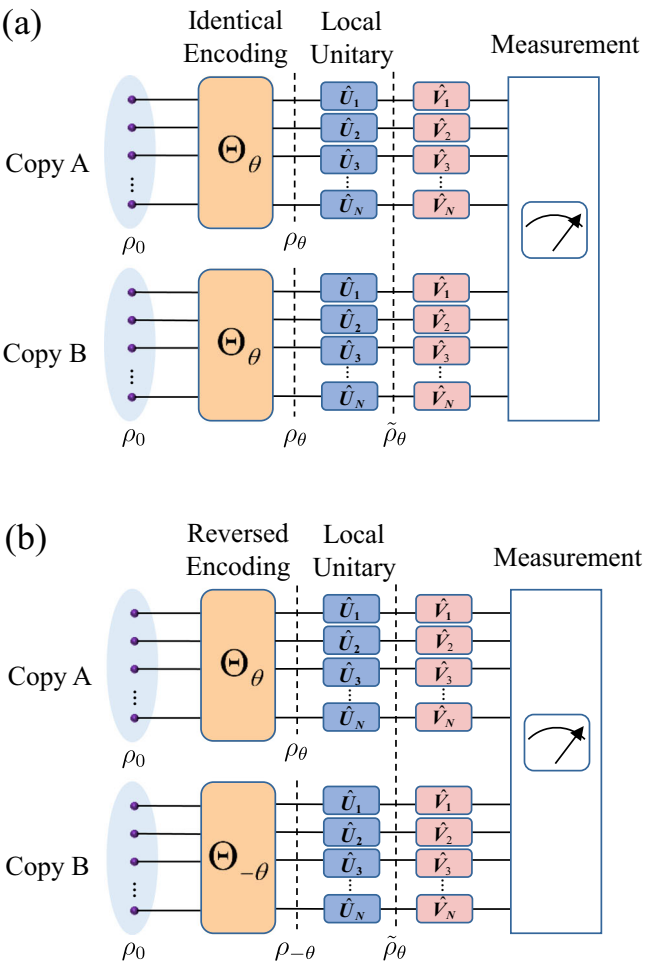

Fig. 2 | Comparison of Encoding Strategies for 2-copy LUI States. a 2-LUI-IE Protocol: Both copies undergo the same encoding operation, Θ_θ, and in this case, only nonlocal interactions can give rise to a non-vanishing QFI. **b** 2-LUI-RE Protocol: The two copies are reversely encoded with Θ_θ and $\Theta_{-\theta}$. This structure explicitly breaks the SWAP symmetry between the copies. Crucially, while Θ_θ is depicted as a global unitary for generality, this strategy is effective even when the encoding is generated by purely local interactions at a single site.

$\Theta_\theta = \exp(-i\theta\sum_i h_i)$ where h_i denotes a local Hamiltonian acting on site i - the 2-Rényi entropy remains independent of θ, and consequently,

$$\mathcal{F}_{2-\mathrm{LUI-IE}} = 0, \textit{ if } \Theta_\theta \text{ is local}. \tag{8}$$

Imai also reaches similar conclusions in[29], which are consistent with the predictions of the no-go theorem.

In the reversed encoding strategy, called 2-LUI-RE protocol, the two copies are encoded oppositely, as shown in Fig. 2(b): $P_\theta = (\Theta_\theta \rho_0 \Theta_\theta^\dagger) \otimes (\Theta_{-\theta} \rho_0 \Theta_{-\theta}^\dagger) = \rho_\theta \otimes \rho_{-\theta}$. For an encoding process $\Theta_\theta = e^{-i\hat{H}\theta}$, its reverse is $\Theta_{-\theta} = e^{i\hat{H}\theta}$.

The reversed operation $\Theta_{-\theta}$ can be realized through several physically relevant methods. In optical systems, such reversal can be achieved by inverting the input-output directions of the encoding black box[37], for instance, by reversing the spatial orientation of the optical crystal. This approach is valid for Hermitian interaction satisfying $\Theta_{-\theta} = \Theta_\theta^\dagger$[38]. For more general configurations with Hamiltonians expressed in terms of Pauli operators, including most atomic spin systems, a reversal can often be implemented via conjugation with other local unitaries. For instance, if $\hat{H} = \frac{1}{2}\sum_{i\in K} Z_i$ on some sites set K,

then applying a Pauli-X operation $X = \bigotimes_{i=1}^{N} X_i$ before and after the encoding achieves the reversal: $\Theta_{-\theta} = X\Theta_\theta X$.

With the help of the reversed encoding and local-twirling, the QFI of the LUI mixed state $\widetilde{\rho}_\theta$ is

$$\mathcal{F}_{2-\mathrm{LUI-RE}} = \frac{1}{2^N}\sum_{\vec{\mathbf{b}}} \frac{\left[\sum_{\vec{\mathbf{a}}}(-1)^{\vec{\mathbf{a}}\cdot\vec{\mathbf{b}}}\partial_\theta Tr(\rho_{\theta,\vec{\mathbf{a}}}\rho_{-\theta,\vec{\mathbf{a}}})\right]^2}{\sum_{\vec{\mathbf{a}}}(-1)^{\vec{\mathbf{a}}\cdot\vec{\mathbf{b}}} Tr(\rho_{\theta,\vec{\mathbf{a}}}\rho_{-\theta,\vec{\mathbf{a}}})}, \tag{9}$$

where $\rho_{-\theta,\vec{\mathbf{a}}} := Tr_{i:a_i=0}(\Theta_{-\theta}\rho_0\Theta_{-\theta}^\dagger)$.

Moreover, for general cases of Θ_θ, at small θ, the mixed state generated by the 2-LUI-RE protocol approaches the QFI of the untwirled pure state P_θ, given by $\mathcal{F}_0(P_\theta) = 8[Tr(\rho_\theta \widehat{H}^2) - Tr(\rho_\theta \widehat{H})^2]$, leading to the asymptotic equivalence:

$$\lim_{\theta\to 0} \mathcal{F}_{2-\mathrm{LUI-RE}} = \mathcal{F}_0. \tag{10}$$

This contrasts starkly with the vanishing QFI in the 2-LUI-IE case, and showcases the optimality of the reversed encoding for small θ. Details of the asymptotic behavior for the 2-LUI-RE protocol are provided in Supplementary Note IV.

Crucially, unlike 2-LUI-IE protocol, $\mathcal{F}_{2-\mathrm{LUI-RE}}$ remains nonzero even when both Θ_θ and $\Theta_{-\theta}$ are generated by a local Hamiltonian of the form $\widehat{H} = \sum_{i\in K} h_i$ with some local Hamiltonian h_i on site i, and site set K. This is because the overlap terms $Tr(\rho_{\theta,\vec{\mathbf{a}}}\rho_{-\theta,\vec{\mathbf{a}}})$ are non-trivially dependent on θ. Here, we are going to give three examples with Pauli Hamiltonian.

Example 1: encodings on one site: $\Theta_\theta = e^{-iZ_1\theta/2}$ with Z_1 is the local Pauli-Z operator at site-1. The QFI is:

$$\mathcal{F}_{2-\mathrm{LUI-RE}}(\rho) = \frac{4\cos^2(\theta)Tr(\rho^2 - Z_1\rho Z_1\rho)}{2 - \sin^2(\theta)Tr(\rho^2 - Z_1\rho Z_1\rho)}, \tag{11}$$

where ρ is an initial encoded pure state. Apparently, for a state ρ with non-trivial initial Fisher information $\mathcal{F}_0 = 2Tr(\rho^2 - Z_1\rho Z_1\rho) \neq 0$, the QFI after twirling is non-trivial. This case proves that our 2-LUI-RE protocol works for local encodings. And for small θ, $\mathcal{F}_{2-\mathrm{LUI-RE}}(\rho)$ is near with $\mathcal{F}_0$; for larger θ, the QFI after twirling may decrease. The derivations are provided in Supplementary Note V.

Example 2: the initial state is the product state. Consider the initial product state $|\psi_{prod}\rangle = \bigotimes_{i=1}^{N}\frac{1}{\sqrt{2}}(|H_i\rangle + |V_i\rangle)$ defined in the local basis $|H_i\rangle$ and $|V_i\rangle$. When we consider the encoding Hamiltonian $\widehat{H} = \frac{1}{2}\sum_i Z_i$, the QFI of the resulting LUI state becomes

$$\mathcal{F}_{2-\mathrm{LUI-RE}}(\psi_{prod}) = \frac{4N\cos^2\theta}{1+\cos^2\theta}. \tag{12}$$

In the small-θ limit, we find $lim_{\theta\to 0}\mathcal{F}_{2-\mathrm{LUI-RE}}(\psi_{prod}) = \mathcal{F}_0(\psi_{prod}) = 2N$, which corresponds to the SQL. The derivations are provided in Supplementary Note V.

Example 3: the initial state is the GHZ state. Now consider the GHZ state in the local basis, $|\psi_{GHZ}\rangle = \frac{1}{\sqrt{2}}(|H_1H_2\cdots H_N\rangle + |V_1V_2\cdots V_N\rangle)$. Still considering the encoding Hamiltonian $\widehat{H} = \frac{1}{2}\sum_i Z_i$, the QFI of the corresponding LUI state is

$$\mathcal{F}_{2-\mathrm{LUI-RE}}(\psi_{GHZ}) = 2N^2[1 - \frac{\sin^2(N\theta)}{\cos^2(N\theta) + 2^{N-1}}]. \tag{13}$$

Taking the limit $\theta \to 0$, we obtain

$$\lim_{\theta\to 0} \mathcal{F}_{2-\mathrm{LUI-RE}}(\psi_{GHZ}) = \mathcal{F}_0(\psi_{GHZ}) = 2N^2, \tag{14}$$

which corresponds to the HL. Importantly, the GHZ state is the optimal probe under local encoding, so the maximal QFI achievable with two independent copies is $\mathcal{F}_{\max} = \mathcal{F}_0(\psi_{GHZ}) = 2N^2$. Hence, even under local operations and reference-frame averaging, our protocol retains Heisenberg scaling. Further details are provided in Supplementary Note V.

These examples clearly indicate that the 2-LUI-RE protocol fully preserves the QFI for small values of θ, while for large values of θ, the protocol's sensitivity can be restored to the optimal level through prior knowledge of the system or by implementing an adaptive measurement scheme.

The IE protocol is doubly-constrained by both RF-invariance and SWAP-symmetry, which significantly restrict its manifold of achievable states to the extent that local operations become insufficient. By relaxing the SWAP-symmetry constraint, the RE protocol targets a larger manifold, where the correlated structure of the $\Theta_\theta \otimes \Theta_{-\theta}$ operation provides the necessary resource to encode information robustly in RF-independent scenarios.

In summary, the 2-LUI-RE protocol offers two significant advantages: (i) it enables metrological usefulness of LUI states under fully local operations, and (ii) it provides robustness against reference-frame misalignment while preserving complete QFI.

Heisenberg-limited distributed phase estimation

In this subsection, we demonstrate the validity of the 2-LUI-RE protocol in a fundamental task of distributed phase estimation: estimating a single collective parameter that depends on independent local parameters θ_i, each accessed by one of N spatially separated local sensors[8–10]. A notable paradigm is a 'world clock' across a network of clocks across the world[4], which can be modeled as a task to estimate the simple average $\overline{\theta} = \frac{1}{N}\sum_i \theta_i$.

Quantum resources, e.g., the GHZ state, offer a dramatic advantage for this task compared to measuring them individually. Remarkably, a network of N entangled quantum sensors can achieve the HL[5–7,39,40], where the precision scales as $1/N$[9]. Suppose the entire network is in a multi-site GHZ state: $|\psi_{GHZ}\rangle = \frac{1}{\sqrt{2}}(|H_1H_2\cdots H_N\rangle + |V_1V_2\cdots V_N\rangle)$ with $|H_i(V_i)\rangle$ for local horizontal (vertical) polarization. Suppose the parameter of interest at each site is imprinted by a locally-trust interaction with Hamiltonian $h_i = \frac{1}{2}Z_i = \frac{1}{2}(|H_i\rangle\langle H_i| - |V_i\rangle\langle V_i|)$. The total encoding operation is the product of all local unitaries: $\Theta_{\vec{\boldsymbol{\theta}}} = \exp(-\frac{i}{2}\sum_j Z_j\theta_j)$. When this operation is applied to the GHZ state, the resulting state is:

$$\Theta_{\vec{\boldsymbol{\theta}}}|\psi_{GHZ}\rangle = \frac{1}{\sqrt{2}}(|H_1\cdots H_N\rangle + e^{iN\overline{\theta}}|V_1\cdots V_N\rangle). \tag{15}$$

The average parameter $\overline{\theta}$ is now encoded as a global phase on the highly sensitive entangled state, which allows it to suit our protocol.

2-LUI-RE protocol uses two copies of the GHZ network state and applies a specific reversed encoding on the second copy before subjecting both to an identical twirling process, as shown in Fig. 3. Given the Eq. (10), this protocol preserves the quantum advantage. The QFI for the final, RF-independent state is:

$$\lim_{\overline{\theta}\to 0} \mathcal{F}_{2-\mathrm{LUI-RE}}(\psi_{GHZ}, \overline{\theta}) = \mathcal{F}_0(\psi_{GHZ}, \overline{\theta}) = 2N^2, \tag{16}$$

which is the original Heisenberg-limited QFI for the ideal GHZ state. This means that even when the sensors have no shared RF, our

protocol allows them to collectively estimate the global average parameter $\bar{\theta}$ with a precision that scales as $1/N$, the full HL.

Optimal measurement strategy

While the QFI quantifies the ultimate precision bound for a quantum state, this bound is achievable only with optimal measurements. According to Eq. (5), the actual estimation precision after measurement is determined by the CFI, defined via the outcome probabilities $\{p_k\}$ as $F=\sum_k(\partial_\theta p_k)^2/p_k$. For our reversed-encoding strategy, the metrological information is contained in the expectation values of local and global SWAP operators, $Tr(\hat{S}_{\vec{\mathbf{a}}}P_\theta)$. The central challenge is therefore to design a measurement strategy that efficiently extracts these values.

One seemingly straightforward approach is direct computational basis measurement (DM) at each site, as depicted in Fig. 4a. This procedure is operationally equivalent to performing local randomized measurements (LRM) on the initial state P_θ, to estimate the cross-copy correlations $Tr(\hat{S}_{\vec{\mathbf{a}}}P_\theta)$[41,42].

Although simple to implement, this method is highly inefficient. Taking the GHZ state with 2-LUI-RE protocol as an example, the resulting CFI is:

$$F^{DM}=\frac{4N^2}{(d+1)^N}\sum_{n=0}^{N}\binom{N}{n}\frac{\cos^2(N\theta)\sin^2(N\theta)}{d^n+(-1)^n\cos^2(N\theta)}. \tag{17}$$

As shown in Fig. 5, DM extracts only a small fraction of the maximum QFI $\mathcal{F}_{\max}$. For large N, the maximum achievable CFI scales as

$$F^{DM}_{\max}\sim\frac{1}{d^N}\mathcal{F}_{\max}\sim\frac{N^2}{d^N}, \tag{18}$$

demonstrating an exponential loss of information and a failure to preserve the HL. A global randomized measurement performs similarly poorly (demonstrated in Supplementary Note VII).

A far more effective strategy is the local SWAP test (LST)[43], which enables explicit extraction of $\langle\hat{S}_{\vec{\mathbf{a}}}\rangle$. As shown in Fig. 4(b), this is implemented by introducing an ancillary qubit at each site and performing control-SWAP operations. The power of this method stems from the invariance of the SWAP operator under the twirling channel: $Tr(\hat{S}_{\vec{\mathbf{a}}}\tilde{\rho}_\theta)=Tr(\hat{S}_{\vec{\mathbf{a}}}\Phi^{(2)}(P_\theta))=Tr(\Phi^{(2)}(\hat{S}_{\vec{\mathbf{a}}})P_\theta)=Tr(\hat{S}_{\vec{\mathbf{a}}}P_\theta)$. Consequently, measuring the ancillary qubits provides direct access to the encoded information. For measurement basis on $\vec{\mathbf{b}}\in[0,1]^N$, the corresponding measurement probabilities $p_{\vec{\mathbf{b}}}=\frac{1}{2^N}\sum_{\vec{\mathbf{a}}}(-1)^{\vec{\mathbf{a}}\cdot\vec{\mathbf{b}}}\langle\hat{S}_{\vec{\mathbf{a}}}\rangle$, yielding a CFI that saturates the QFI:

$$F^{LST}=\mathcal{F}_{2-\mathrm{LUI-RE}},\ lim_{\theta\to0}F^{LST}=\mathcal{F}_0. \tag{19}$$

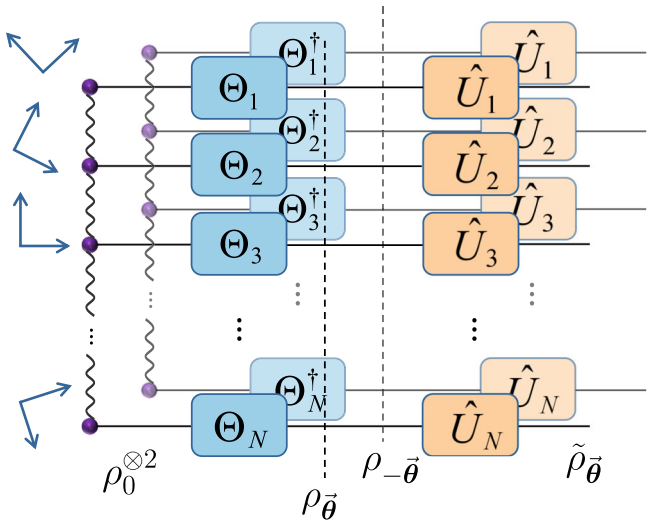

Fig. 3 | 2-LUI-RE Protocol with Independent Encodings. Two copies of the GHZ state (ρ_0) are shared by separated sites in a network, and then each site applies reversed-encoding on two on-hand photons with opposing encoding Θ_i and $\Theta_i^\dagger$, forming two reversely encoded network states $\rho_{\vec{\boldsymbol{\theta}}}$ and $\rho_{-\vec{\boldsymbol{\theta}}}$. Afterward, each site performs local randomized rotations $\hat{U}=\bigotimes_{i=1}^N\hat{U}_i$ to the two photons to generate the LUI state $\tilde{\rho}_{\vec{\boldsymbol{\theta}}}$. The averaged parameter $\bar{\theta}=\frac{1}{N}\sum_{i=1}^N\theta_i$ can be estimated through a specific measurement strategy geared toward $\tilde{\rho}_{\vec{\boldsymbol{\theta}}}$.

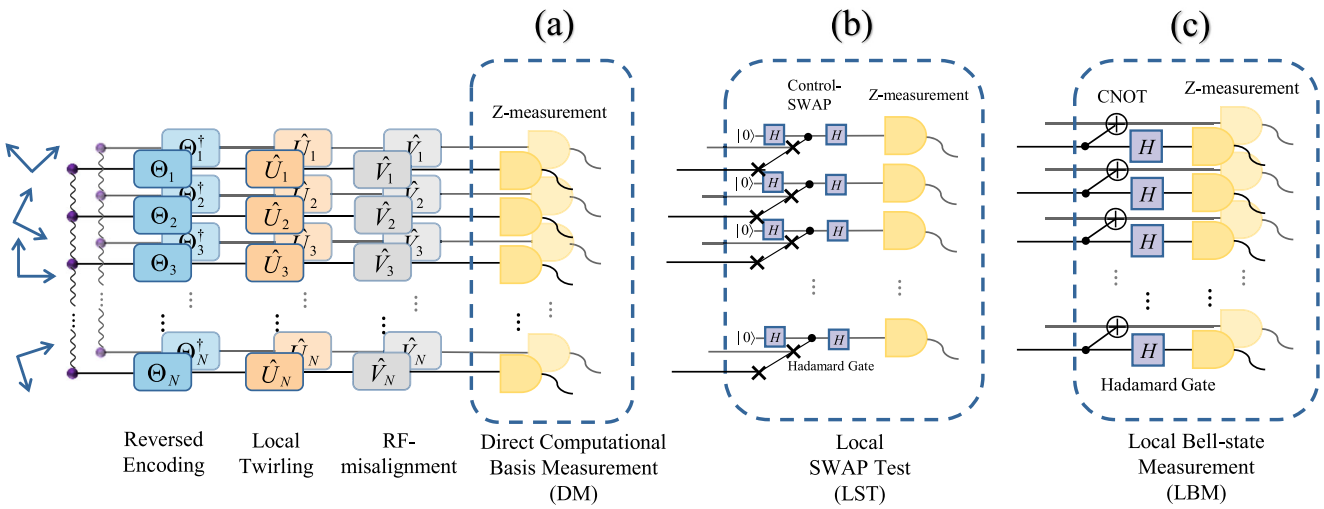

Fig. 4 | Local Measurement Strategies for the 2-LUI-RE Protocol. a Direct Computational Basis Measurement (DM). Each qudit is measured directly in the computational basis. This strategy suffers an exponential loss of information. **b** Local SWAP Test (LST). An ancillary qubit is introduced at each site to perform a controlled-SWAP operation between the two copies. **c** Local Bell-state Measurement (LBM). For qubit systems ($d=2$), the local SWAP test is operationally equivalent to a Bell-state measurement. This is implemented efficiently using a CNOT gate and a Hadamard gate at each site, followed by Z-basis measurements. LST and LBM constitute optimal measurement strategies.

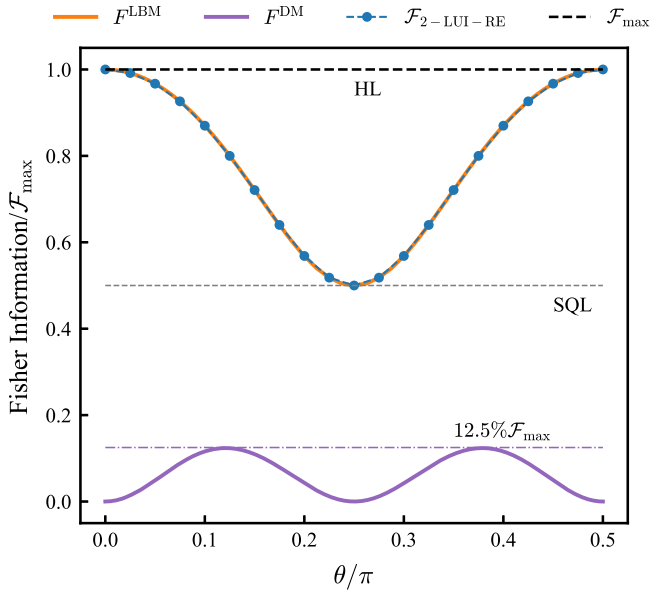

Fig. 5 | Fisher Information for Different Measurement Strategies in the 2-LUI-RE Protocol. The QFI of the protocol (blue dashed-dotted line) represents the ultimate precision bound. The CFI from the optimal LBM (orange solid line) perfectly saturates the Cramér-Rao bound, while the CFI from a naive DM (purple solid line) performs dramatically worse, falling far below the SQL.

Especially, for qubit systems ($d = 2$), this protocol can be simplified further. Each local SWAP test is operationally equivalent to a local Bell-state measurement, which can be implemented without ancillary systems using CNOT and Hadamard gates (Fig. 4(c)), which projects the two on-hand photons onto the Bell singlet state, $\frac{1}{\sqrt{2}}(|H_iV_i\rangle - |V_iH_i\rangle)$ and its orthogonal complement. With this optimal strategy, the gathered CFI matches that of the reversed-encoding LUI state:

$$F^{\mathrm{LBM}} = \mathcal{F}_{2-\mathrm{LUI}-\mathrm{RE}},\ lim_{\theta\to 0}F^{\mathrm{LBM}} = \mathcal{F}_0. \tag{20}$$

The stark difference in the efficacy of these measurement strategies is quantified in Fig. 5. The simulation considers an initial $N = 2$ GHZ state and an encoding Hamiltonian $\widehat{H} = \frac{1}{2}\sum Z_i$. The dashed-dotted blue line shows the QFI of our 2-LUI-RE state ($\mathcal{F}_{2-\mathrm{LUI}-\mathrm{RE}}$). Crucially, the solid orange line (F^{LBM}) shows the CFI extracted using our proposed LBM strategy. It perfectly overlaps with the QFI, proving that LBM is an optimal measurement that saturates the QCRB for all values of θ. When θ is small, the HL scaling is achieved and for large θ, we could still extract most of the Fisher information with LBM. In stark contrast, the solid purple line (F^{DM}) represents the CFI from a direct computational basis measurement. This simple approach is highly inefficient, peaking at only 12.5% of the maximum possible information. This performance gap between the optimal LBM and the naive DM becomes larger with the number of particles N, underscoring the critical importance of employing the correct measurement strategy to preserve the quantum advantage in distributed sensing. Further details are provided in Supplementary Note VII.

Discussion

Our 2-LUI-RE approach circumvents the no-go theorem on distributed quantum sensing. The reversed encoding breaks the SWAP symmetry between copies and retains the full QFI with local Hamiltonians. Furthermore, we have identified an optimal measurement strategy—local SWAP test or local Bell-state measurements—that can extract this information completely, achieving the HL without requiring shared RF or non-local interactions between sites.

From a practical standpoint, the protocol is experimentally feasible. Preparing the required 2-copy LUI states is straightforward. For qubit systems, local Clifford operations suffice, and for general k-copy states, the twirling can be efficiently approximated using unitary k-designs, greatly reducing experimental complexity.

In conclusion, we have presented a comprehensive and experimentally viable solution to the deadlocks of distributed quantum sensing in the absence of a shared RF. By simultaneously overcoming the pervasive decoherence effects of RF misalignment and the fundamental limitations on local encoding, our work paves the way for practical implementations of high-precision, networked quantum technologies.

Data availability

Authors can confirm that all relevant data are included in the paper and/or its supplementary information files.

References

1. Bartlett, S. D., Rudolph, T. & Spekkens, R. W. Reference frames, superselection rules, and quantum information. *Rev. Mod. Phys.* **79**, 555 (2007).
2. Kovalevsky, J., Mueller, I. I. & Kolaczek, B. Reference frames: in astronomy and geophysics, Vol. 154 (Springer, 2012).
3. Quirrenbach, A. Optical interferometry. *Annu. Rev. Astron. Astrophys.* **39**, 353 (2001).
4. Kómár, P. et al. A quantum network of clocks. *Nat. Phys.* **10**, 582 (2014).
5. Guo, X., Breum, C. R., Borregaard, J., Izumi, S. & Andersen, U. L. Distributed quantum sensing in a continuous-variable entangled network. *Nat. Phys.* **16**, 1 (2020).
6. Zhao, S. R. et al. Field demonstration of distributed quantum sensing without post-selection. *Phys. Rev. X* **11**, 031009 (2021).
7. Liu, L. Z., Zhang, Y. Z., Li, Z. D., Zhang, R. & Pan, J. W. Distributed quantum phase estimation with entangled photons. *Nat. Photon.* **15**, 137 (2021).
8. Proctor, T. J., Knott, P. A. & Dunningham, J. A. Multiparameter estimation in networked quantum sensors. *Phys. Rev. Lett.* **120**, 080501 (2018).
9. Ge, W., Jacobs, K., Eldredge, Z., Gorshkov, A. V. & Foss-Feig, M. Distributed quantum metrology with linear networks and separable inputs. *Phys. Rev. Lett.* **121**, 043604 (2018).
10. Gessner, M., Pezzè, L. & Smerzi, A. Sensitivity bounds for multiparameter quantum metrology. *Phys. Rev. Lett.* **121**, 130503 (2018).
11. Yang, Y., Yadin, B. & Xu, Z.-P. Quantum-enhanced metrology with network states. *Phys. Rev. Lett.* **132**, 210801 (2024).
12. Marvian, I. Restrictions on realizable unitary operations imposed by symmetry and locality. *Nat. Phys.* **18**, 283 (2022).
13. Giovannetti, V., Lloyd, S. & Maccone, L. Quantum-enhanced measurements: beating the standard quantum limit. *Science* **306**, 1330 (2004).
14. Giovannetti, V., Lloyd, S. & Maccone, L. Quantum metrology. *Phys. Rev. Lett.* **96**, 010401 (2006).
15. PARIS, M. G. A. Quantum estimation for quantum technology. *Int. J. Quantum Inform.* **07**, 125 (2009).
16. Giovannetti, V., Lloyd, S. & Maccone, L. Advances in quantum metrology. *Nat. Photon.* **96**, 222 (2011).
17. Tóth, G. & Apellaniz, I. Quantum metrology from a quantum information science perspective. *J. Phys. A Math. Theor.* **47**, 424006 (2014).
18. Dowling, J. P. & Seshadreesan, K. P. Quantum optical technologies for metrology, sensing, and imaging. *J. Lightw. Technol.* **33**, 2359 (2015).
19. Pezzè, L., Smerzi, A., Oberthaler, M. K., Schmied, R. & Treutlein, P. Quantum metrology with nonclassical states of atomic ensembles. *Rev. Mod. Phys.* **90**, 035005 (2018).

20. Braun, D. et al. Quantum-enhanced measurements without entanglement. *Rev. Mod. Phys.* **90**, 035006 (2018).
21. Pirandola, S., Bardhan, B. R., Gehring, T., Weedbrook, C. & Lloyd, S. Advances in photonic quantum sensing. *Nat. Photon.* **12**, 724 (2018).
22. Escher, B. M., de Matos Filho, R. L. & Davidovich, L. General framework for estimating the ultimate precision limit in noisy quantum-enhanced metrology. *Nat. Phys.* **7**, 406 (2011).
23. Demkowicz-Dobrzański, R., Kołodyński, J. & Guţă, M. The elusive heisenberg limit in quantum-enhanced metrology. *Nat. Commun.* **3**, 1063 (2012).
24. Len, Y. L., Gefen, T., Retzker, A. & Kołodyński, J. Quantum metrology with imperfect measurements. *Nat. Commun.* **13**, 6971 (2022).
25. Arrad, G., Vinkler, Y., Aharonov, D. & Retzker, A. Increasing sensing resolution with error correction. *Phys. Rev. Lett.* **112**, 150801 (2014).
26. Kessler, E. M., Lovchinsky, I., Sushkov, A. O. & Lukin, M. D. Quantum error correction for metrology. *Phys. Rev. Lett.* **112**, 150802 (2014).
27. Dür, W., Skotiniotis, M., Froewis, F. & Kraus, B. Improved quantum metrology using quantum error correction. *Phys. Rev. Lett.* **112**, 080801 (2014).
28. Zhou, S., Zhang, M., Preskill, J. & Jiang, L. Achieving the heisenberg limit in quantum metrology using quantum error correction. *Nat. Commun.* **9**, 78 (2018).
29. Imai, S., Gühne, O. & Tóth, G. Reference-frame-independent quantum metrology, https://arxiv.org/abs/2410.10518 arXiv:2410.10518 (2024).
30. Born, M. & Wolf, E. Principles of optics: electromagnetic theory of propagation, interference and diffraction of light (Elsevier, 2013).
31. d'Alessandro, D. *Introduction to quantum control and dynamics* (Chapman and Hall/CRC, 2021).
32. Elben, A. et al. The randomized measurement toolbox. *Nat. Rev. Phys.* **5**, 9–24 (2022).
33. Elben, A., Vermersch, B., Roos, C. F. & Zoller, P. Statistical correlations between locally randomized measurements: A toolbox for probing entanglement in many-body quantum states. *Phys. Rev. A* **99**, 052323 (2019).
34. Zhang, L. Matrix integrals over unitary groups: An application of schur-weyl duality, arXiv:1408.3782 https://arxiv.org/abs/1408.3782 (2014).
35. Pang, S. & Brun, T. A. Quantum metrology for a general hamiltonian parameter. *Phys. Rev. A* **90**, 022117 (2014).
36. Liu, J., Chen, J., Jing, X.-X. & Wang, X. Quantum fisher information and symmetric logarithmic derivative via anti-commutators. *J. Phys. A: Math. Theor.* **49**, 275302 (2016).
37. Chiribella, G. & Liu, Z. Quantum operations with indefinite time direction. *Commun. Phys.* **5**, 190 (2022).
38. Guo, Y. et al. Experimental demonstration of input-output indefiniteness in a single quantum device. *Phys. Rev. Lett.* **132**, 160201 (2024).
39. Kim, D.-H. et al. Distributed quantum sensing of multiple phases with fewer photons. *Nat. Commun.* **15**, 266 (2024).
40. Malia, B. K., Wu, Y., Martínez-Rincón, J. & Kasevich, M. A. Distributed quantum sensing with mode-entangled spin-squeezed atomic states. *Nature* **612**, 661 (2022).
41. Elben, A. et al. Cross-platform verification of intermediate scale quantum devices. *Phys. Rev. Lett.* **124**, 010504 (2020).
42. Brydges, T. et al. Probing rényi entanglement entropy via randomized measurements. *Science* **364**, 260 (2019).
43. Buhrman, H., Cleve, R., Watrous, J. & de Wolf, R. Quantum fingerprinting. *Phys. Rev. Lett.* **87**, 167902 (2001).

Acknowledgements

We thank You Zhou for the helpful discussion. This work was supported by the National Natural Science Foundation of China (Grant Nos. 12350006, 92576202), Quantum Science and Technology-National Science and Technology Major Project (Nos. 2021ZD0301200), and USTC Research Funds of the Double First-Class Initiative (Grant No. YD2030002026).

Author contributions

H.Q.X. and G.C.L. contributed to the framework formulation, the calculation and derivation of key equations, paper writing, and revisions. G.C. contributed to the paper writing and revision. X.S.H., L.C., SQ.Z., and Y.L., contributed to the discussion. G.C., CF.L., and GG.C. supervised the work.

Competing interests

The authors declare no competing interests.

Additional information

Supplementary information The online version contains supplementary material available at https://doi.org/10.1038/s41467-025-67771-9.

Correspondence and requests for materials should be addressed to Geng Chen.

Peer review information *Nature Communications* thanks the anonymous reviewers for their contribution to the peer review of this work. A peer review file is available.